THE JOURNAL OF PHYSICAL CHEMISTRY A
A JOURNAL OF THE AMERICAN CHEMICAL SOCIETY

pubs.acs.org/JPCA

Article

Reactive Uptake of Hydroperoxymethyl Thioformate to Sodium Chloride and Sodium Iodide Aerosol Particles

Published as part of The Journal of Physical Chemistry virtual special issue "Advances in Atmospheric Chemical and Physical Processes".

Christopher M. Jernigan, Christopher D. Cappa, and Timothy H. Bertram*

Cite This: https://doi.org/10.1021/acs.jpca.2c03222

Read Online

ACCESS | Metrics & More | Article Recommendations

ABSTRACT: The oxidation products of dimethyl sulfide (DMS) contribute to the production and growth of cloud condensation nuclei (CCN) in the marine boundary layer. Recent work demonstrates that DMS is oxidized by OH radicals to the stable intermediate hydroperoxymethyl thioformate (HPMTF), which is both globally ubiquitous and efficiently lost to multiphase processes in the marine atmosphere. At present, there are no experimental measurements of the reactive uptake of HPMTF to aerosol particles, limiting model implementation of multiphase HPMTF chemistry. Using an entrained aerosol flow reactor combined with chemical ionization mass spectrometry (CIMS), we measured the reactive uptake coefficient (γ) of HPMTF to dry sodium chloride (NaCl), wet NaCl, and wet sodium iodide (NaI) particles to be $(1.9 \pm 1.3) \times 10^{-4}$, $(1.6 \pm 0.6) \times 10^{-3}$, and $(9.2 \pm 2.3) \times 10^{-1}$, respectively. While we did not directly measure the condensed-phase products of HPMTF reactive uptake in this experiment, the ionization products observed in the CIMS instrument provide mechanistic insight on the reaction mechanism of HPMTF with halides.

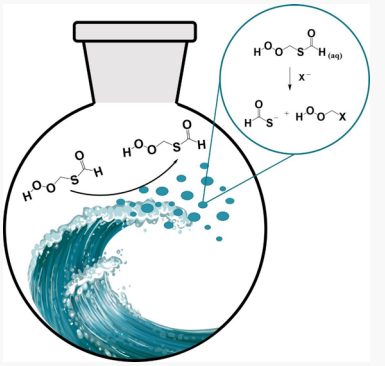

INTRODUCTION

Dimethyl sulfide (DMS) is a biogenically produced molecule emitted primarily from the ocean and is a significant source of reduced sulfur to the atmosphere.[1,2] Once emitted, DMS is primarily oxidized by OH and BrO radicals, leading ultimately to the formation of both low volatility, water-soluble oxidation products (e.g., sulfuric acid and methanesulfonic acid) and long-lived sulfur reservoir species (e.g., carbonyl sulfide). Until recently, it was thought that DMS was mainly oxidized to sulfur dioxide (SO_2) and methanesulfonic acid (MSA) at high yield, where SO_2 can be further oxidized to sulfuric acid (H_2SO_4) leading to new particle formation while MSA condenses to existing particle resulting in particle growth. As a result, the mechanism by which DMS is oxidized determines the formation and growth rates of aerosol particles to cloud condensation nuclei (CCN) sizes in marine environments, with consequent effects on Earth's radiative budget.[3−5] The aerosol radiative forcing by natural aerosols, such as DMS-derived aerosol particles, accounts for the largest uncertainty in radiative forcing in climate models.[6]

Recent computational, laboratory, and field-studies have shown that the textbook representation of DMS oxidation by OH radicals is incomplete.[7−10] Specifically, it is now understood that the primary peroxy radical formed from the OH-initiated oxidation of DMS, methylthiomethyl peroxy radical (MTMP, $CH_3SCH_2OO^{\bullet}$), can rapidly isomerize via a unimolecular 2-step hydrogen shift reaction to form the stable product hydroperoxymethyl thioformate (HPMTF; $HOOCH_2SCHO$). Isomerization competes with reaction of MTMP with other species, such as NO, but in the marine environment it is estimated that >45% of emitted DMS goes on to form HPMTF,[8,10−12] resulting in HPMTF being globally ubiquitous.[7] Recent laboratory measurements have found that the gas phase loss of HPMTF to OH is relatively slow ($k_{HPMTF+OH} = 1.4 \times 10^{-11}$ cm^3 molecule^{-1} s^{-1}) allowing multiphase pathways to contribute substantially to the loss of HPMTF the marine atmosphere.[9−11] Multiphase loss processes include dry deposition, reactive uptake to aerosol particles, and cloud loss. When multiphase loss processes are included, global model simulations predict a 35% decrease in global SO_2 production and a 92% decrease in global OCS production from DMS oxidation.[9−11] However, the condensed phase chemistry included in these models is largely unconstrained owing to a lack of direct laboratory measurements of HPMTF uptake coefficients.

Received: May 9, 2022
Revised: June 14, 2022

In the absence of laboratory measurements of HPMTF multiphase chemistry, global models have used a range of reasonable reactive uptake coefficients for HPMTF ($0.001 < \gamma(\mathrm{HPMTF}) < 0.03$) derived from structurally similar molecules.[10,12,13] Here, we present laboratory measurements of the reactive uptake of HPMTF to sodium chloride (NaCl) and sodium iodide (NaI) using an entrained aerosol flow reactor combined with chemical ionization mass spectrometry (CIMS). Observations of HPTMF fragmentation within the CIMS instrument under controlled collisional energies are used to make inferences about the condensed phase oxidation mechanism of HPMTF on sea salt aerosol.

METHODS

Generation and Detection of Aerosol Particles and HPMTF. Aerosol particles were generated with a constant output atomizer (TSI Inc., Model 3076) from dilute solutions (ca. 0.5 wt %) of sodium chloride (Sigma-Aldrich, >99.0% purity) and sodium iodine (Sigma-Aldrich, >99.0% purity). The wet aerosol stream was passed through one or more diffusion dryers to condition the aerosol flow to a known relative humidity (RH). As discussed below, γ(HPMTF) was calculated from the dependence of the HPMTF loss rate to the aerosol surface area concentration ($(0-2) \times 10^5$ μm^2 cm^{-3}). The number concentration of aerosol particles within the flow reactor was modulated by directing a variable fraction of the aerosol flow through either a high-efficiency particulate air filter (PALL, PN 12144) or an unfiltered bypass line.[14] HPMTF was quantified using a Compact Time of Flight (C-ToF) Chemical Ionization Mass Spectrometer utilizing iodine ion chemistry.[7] Particle size distributions and total surface area concentrations (S_a) of the aerosol particles were measured with a Scanning Electrical Mobility Sizer (SEMS, Model 2002 μ_BI) and the total aerosol number concentration was verified by comparison with a water-based Condensation Particle Counter (CPC, TSI Model 3787). To account for the difference in relative humidity and subsequent aerosol size distribution of the particles in the flow reactor (30−50% RH) and the SEMS (~10% RH), a particle growth factor was applied to the total aerosol size distribution using the assumption of spherical dry particles. Growth factors for NaCl and NaI particles were taken from Laskina et al.[15] and Minambres et al.,[16] respectively.

Calculation of the HPMTF Reactive Uptake Coefficient. The reactive uptake of HPMTF to aerosol particles was measured at ambient temperature (298 K) and ~1 atm of synthetic zero air (80% N_2, 20% O_2) in a 79 cm cylindrical glass bulk flow reactor (7.6 cm ID) coated in halocarbon wax (Halocarbon, Halocarbon wax series 600) with an average reaction time of 50.5 ± 7.7 s. The reaction time of the flow reactor is determined by the inlet flow rate of the instruments and an additional diaphragm pump used to set the total flow through the reactor (4.15 standard liters per minute, SLPM). The relative humidity of the aerosol + HPMTF stream was measured by an RH probe (Vaisala, Model HMP110) at the end of the flow reactor. At present, there is no reported organic synthesis of HPMTF, thus a pure source of HPMTF is not commercially available for experimentation. A steady source of HPMTF in air ([HPMTF] = 450−550 ppt) was generated from the OH-initiated oxidation of DMS within a 0.6 m^3 PTFE environmental chamber run under a continuous flow mode at ambient temperature and 1 atm of synthetic, dry zero air, as described in Jernigan et al.[9] The relative humidity of the flow reactor was set by the ratio of a humified aerosol flow (RH > 80%) and the dry flow of the HPMTF source flow (RH < 1%). Fine tuning of the reactor RH was done by supplementing humified zero air to the inlet of the flow reactor, keeping the total flow at 4.15 SLPM. By varying the number of diffusion dryers, the age of the dryers, and the volumetric flow of the supplemental humidified air, a range of flow reactor RH was achieved (30−50% RH).

The following expressions was used to derive the pseudo-first-order rate coefficient for reactant gas loss to particles (k_{het})[14] (E3):

$$\ln([\mathrm{HPMTF}]_i) = \ln([\mathrm{HPMTF}]_f^{w/NaX}) + (k_{wall} + k_{het})\cdot\Delta t \quad \text{(E1)}$$

$$\ln([\mathrm{HPMTF}]_i) = \ln([\mathrm{HPMTF}]_f^{w/oNaX}) + (k_{wall})\cdot\Delta t \quad \text{(E2)}$$

$$k_{het} = \left(\frac{1}{\Delta t}\right)\ln\left(\frac{[\mathrm{HPMTF}]_f^{w/oNaX}}{[\mathrm{HPMTF}]_f^{w/NaX}}\right) \quad \text{(E3)}$$

where $[\mathrm{HPMTF}]_i$, $[\mathrm{HPMTF}]_f^{w/oNaX}$, and $[\mathrm{HPMTF}]_f^{w/NaX}$, are the concentrations of a HPMTF entering the flow reactor, exiting the flow reactor without NaX (X = Cl^-, I^-) particles present, and exiting the flow reactor with NaX particles present, respectively. k_{wall}, k_{het}, and Δt refer to the unimolecular loss rate constant with the wall (units of s^{-1}), the pseudo-first-order rate coefficient for reactant gas loss to particles (units of s^{-1}), and the average reaction time within the flow reactor (units of s), respectively.

The observed first-order rate coefficient for reactant gas loss to particles can also be written as a function of the particle surface area and dependent on the reactive uptake of the gas to a surface (E4):

$$k_{het}(S_a) = \frac{\omega\cdot\gamma}{4} \times S_a \quad \text{(E4)}$$

where S_a is the total surface area of the aerosol stream per unit volume ($(0-2) \times 10^{-3}$, units of cm^{-1}), ω is the mean molecular speed of HPMTF (2.6×10^4, units of cm s^{-1}), and γ is the measured uptake coefficient (unitless). A linear regression of k_{het} and aerosol surface area yields a slope of $((\omega\cdot\gamma)/4)$. The absolute sensitivity of the HPMTF is not required for the calculation of the reactive uptake as the equation relies on the ratio of the HPMTF concentrations with and without aerosol. In terms of I^- CIMS sensitivity, previous studies have found the $I:I^\bullet H_2O$ ratio, that is the relationship between the intensity of the iodide ion (127 m/Q) to that of the iodide water cluster (145 m/Q), has a strong effect on the absolute sensitivity of the species of interest.[13] Over the course of multiple experiments, the $I:I^\bullet H_2O$ ratio was consistent (<2% change) for experiments of a target RH. The CIMS sensitivity to HPMTF was assumed to be constant over a given experiment as long as the $I:I^\bullet H_2O$ ratio remained constant.

RESULTS AND DISCUSSION

Reactive Uptake of HPMTF. The response of HPMTF to changes in particle surface area for a representative experiment is shown in Figure 1. Results from the HPMTF uptake experiments are shown in Figure 2, where individual k_{het} is plotted against the measured S_a at the end of the flow reactor. Each k_{het} data point was calculated using E3, where

https://doi.org/10.1021/acs.jpca.2c03222
J. Phys. Chem. A XXXX, XXX, XXX−XXX

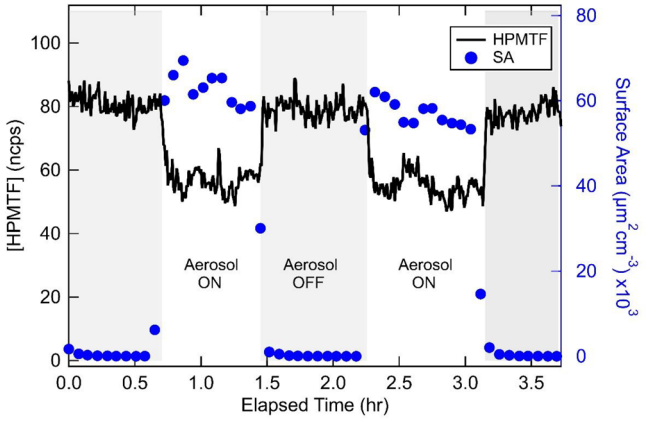

Figure 1. HPMTF (black trace) and total aerosol surface area (blue circles) measured at the base of the flow reactor during a representative experiment at 50.5% RH where particles are modulated on (white section) and off (gray section) using a high-efficiency particulate air filter.

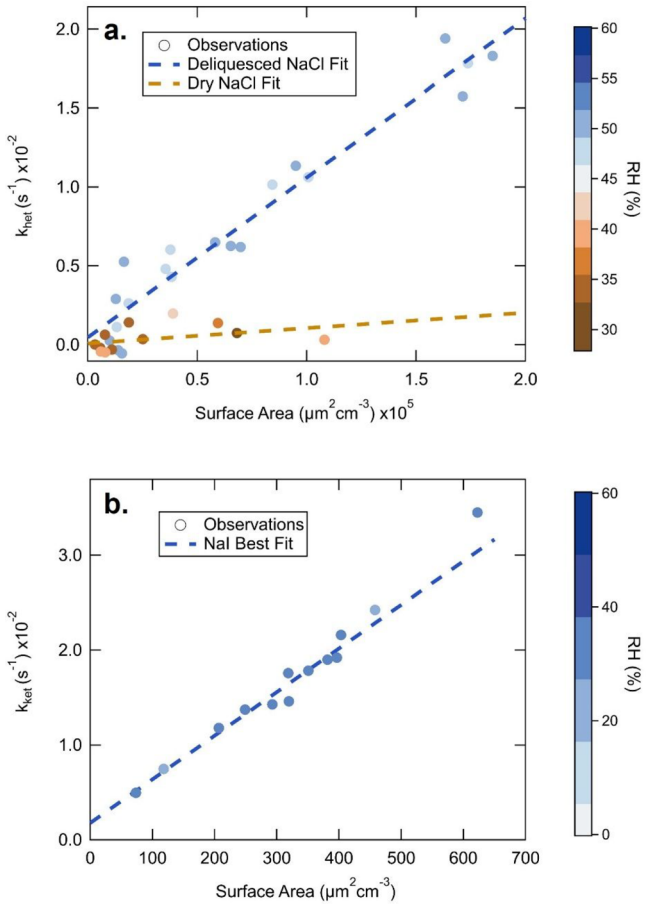

Figure 2. Measured pseudo first-order rate coefficients (k_{het}) for the loss of HPMTF to dry sodium chloride (NaCl) (a, <43%RH), wet NaCl (a, >43%RH), and wet sodium iodide (b, NaI > 0%RH) particles as a function of particle surface area concentration. The color bar indicates the measured relative humidity within the flow reactor with the white section denoting the efflorescence relative humidity for NaCl (a) and NaI (b). The dashed lines represent least-squares fits of the observed data points.

$[HPMTF]_f^{w/oNaX}$ and $[HPMTF]_f^{w/NaX}$ are determined for each S_a concentration. The average residence time (Δt) within the flow reactor, used in E3, was 50.5 ± 7.7 s as discussed above. This was determined using the delay time between the removal or addition of the aerosols within the flow reactor and the detection of a change in the signal of HPMTF and I_2, a product of O_3 and NaI aerosol. The experimental derived Δt was used to approximate the uncertainty in the average residence time HPMTF. As seen in E4, the slope of the regression of k_{het} on S_a is a direct observation of the reactive uptake of HPMTF (γ_{HPMTF}) onto NaCl and NaI aerosols (Figure 2). Experimental points were removed from the regression when large differences in the residence time (due to inlet clogging) and RH (>5% RH), were observed between the particle on and particle off states. Significant changes in the residence time and RH within a step could result in deviations in Δt and k_{wall}, that are required to be constant in E1 and E2.

HPMTF Uptake to NaCl Aerosol Particles. For the NaCl uptake experiments, two RH values, indicative of an RH above and below the efflorescence point of NaCl (43% RH),[17−19] were explored to determine the role of particle liquid water (Figure 2). The hygroscopic growth factor for NaCl ranges from about 1.4 at 43% RH (the ERH) to 1.6 at 60% RH. These correspond to increases in surface area of factors of 1.96 to 2.56 over the dry particles (measured at 10% RH).[17−19] At a relative humidity >43%, k_{het} was strongly correlated with S_a (R^2 = 0.94), resulting in a calculated reactive uptake coefficient (γ) of (1.6 ± 0.6) × 10^{-3}. In contrast, observations at RH < 43% yielded a reactive uptake coefficient of (1.9 ± 1.3) × 10^{-4}. The enhanced γ on effloresced compared to dry NaCl aerosols implies that HPMTF's solubility and hydrolysis reactions play a role in the uptake of HPMTF. No detectable gas-phase products of the HPMTF reaction were detected with the I^- CIMS.

HPMTF Uptake to NaI Aerosol Particles. The NaI uptake experiments were only performed at a single relative humidity, as pure NaI particles remain hydrated at all relative humidity values considered here.[20] A reactive uptake coefficient of (9.2 ± 2.3) × 10^{-1} was determined from the linear regression. The observed increase in HPMTF uptake, relative to NaCl, implies an increased chemical reactivity of HPMTF with NaI. As HPMTF's solubility and hydrolysis would be similar under similar RH values and aerosol phase state, chemical reactions involving iodine are likely driving the increased loss compared to uptake on NaCl. When reactions at the aerosol surface are fast, gas-phase diffusion can be the rate limiting factor in the observed loss.[21,22] To account for the impact of diffusion limitations on our measured uptake coefficient (γ_{exp}), we corrected γ for the NaI experiments using the approach outlined by Hanson and Kosciuch (2003).[22] Using our observed average log-normal particle size distribution with a radius (r_p) of 32 nm and width (ln σ) of 0.61, we calculate and apply a gas-diffusion correction coefficient ($\lambda(\overline{r_s})$) of 0.3 to determine the actual value of γ (E5).

$$\frac{1}{\gamma} = \frac{1}{\gamma_{exp}} - \lambda(\overline{r_S}) \quad \text{(E5)}$$

The only gas-phase product observed was I_2 (detected as $[I_3]^-$ at 381 m/Q) following the addition of NaI particles to the flow reactor. While previous work has found reactions of iodide with ROOH species can liberate I_2.[23] isolation of this path is difficult given the efficient production of I_2 from the reaction of ozone with I^-.[24] Based on the concentration of I_2,

https://doi.org/10.1021/acs.jpca.2c03222
J. Phys. Chem. A XXXX, XXX, XXX−XXX

we expect that most (if not all) of the I_2 production arises from the reaction of ozone (present within the HPMTF flow at concentrations of 50−80 ppb) with iodide anions either on the reactor wall or in the suspended particles.[25]

Insight into HPMTF Condensed Phase Reactions. The dependence of γ(HPMTF) on halide speciation suggests that HPMTF reacts preferentially with I^- compared with Cl^-, and HPMTF uptake is not driven solely by solubility and hydrolysis reactions. The differing halide reactivity toward peroxide oxidation or nucleophilic substitution at the carbonyl functional groups of HPMTF could explain the difference in reactive uptake.[23,26] While we did not directly measure the products of HPMTF multiphase chemistry, we can consider the product ion distribution in the CIMS to discern the dominant reaction pathways for HPMTF in small halide−water clusters. The CIMS can be operated either using I^- (the default operating condition) or Cl^- as the reagent ion, and these are predominately observed as $X^-(H_2O)_n$ clusters with HPMTF detected as $X^-(HPMTF)(H_2O)_n$.[27] The reactivity of HPMTF in these small halide−water clusters provides insight into how HPMTF might react with hydrated NaI and NaCl particles. Experimentally, by changing the collisional energy imparted on the $X^-(HPMTF)(H_2O)_n$ cluster in the CIMS to induce dissociation of the cluster, we can identify whether a reaction has occurred in the cluster within the CIMS. It is important to note that the added collisional energy is not large enough to induce a chemical reaction, just to break apart the ion-neutral cluster. This is accomplished in the CIMS by scanning the electric field at the entrance to one of the focusing quadrupoles.[28,29] In the absence of a reaction, the $X^-(HPMTF)(H_2O)_n$ cluster will dissociate to X^-, H_2O, and neutral HPMTF and no new product ion will be observed. If a reaction has occurred in the $X^-(HPMTF)(H_2O)_n$ cluster, we would observe a commensurate increase in a product ion signal with the decrease in $X^-(HPMTF)$ signal.

When scans were run using either ionization modes, a dominant peak at 235 m/z and 143 m/z was identified and attributed to a HPMTF cluster with iodine and chloride, respectively. Under both ionization modes, we observe an increase in the intensity of $CHOS^-$ (61 m/z) as the declustering voltage was increased within the CIMS instrument and that corresponds to a decrease in the HPMTF cluster signal (Figure 3). The change in the measured CIMS ion intensity was not conserved in the experiment, where we measure a 2 ncps decrease in $I^-(HPMTF)$ compared to a to 1 ncps increase in $CHOS^-$ for the iodine CIMS. A similar result was found for the Cl^- CIMS experiment. This discrepancy could be due to differences in the transmission of the two ions, dissociation of HPMTF into minor fragments, or declustering of $I^-(HPMTF)$ into a neutral HPMTF + I^-. Nonetheless, for both I^- and Cl^-these results provide evidence that HPMTF reacts with halide ions, at least in these small clusters, to produce some new product (here, detected as $CHOS^-$).

While we did not directly probe the condensed phase reaction of HPMTF, the CIMS product ion distribution provides insight into the outcome of a reaction between HPMTF and a halide ion in a small cluster. To explain the formation of the $CHOS^-$ ion, we suggest a substitution like reaction between the reagent ion and HPMTF:

$$[X]^- + HOOCH_2SCHO \rightarrow [X^{\bullet}HOOCH_2SCHO]^- \rightarrow HOOCH_2X + [SCHO]^- \quad X = I, C \qquad (E6)$$

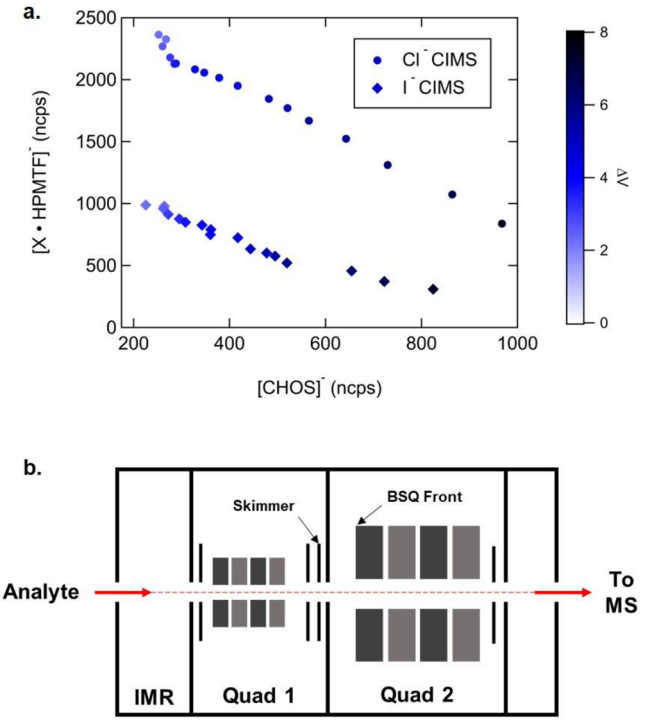

Figure 3. Relationship between the intensity of the reagent ion (Iodide in diamonds and Chloride in circles) clustered with HPMTF $[X^{\bullet}HPMTF]^-$ (at 235 and 143 m/z, respectively) and the ion $[CHSO]^-$ (at 61 m/z) as a function of the magnitude of the declustering voltage represented by the colorbar (top panel). A schematic of the C-ToF instrument with the skimmer and big segmented quadrupole (BSQ) front voltages labeled to represent the declustering region (bottom panel). Halide clusters are formed in the ion molecule region (IMR) and guided to the mass analyzer (MS) through two focusing quadrupole regions (Quads 1 and 2).

If HPMTF reacts in a similar way with a hydrated ion either at the surface or in the bulk of an aqueous aerosol, this analysis suggests that HPMTF may form $CHOS^-$ as the first-generation product. It is not yet clear what the condensed-phase fate of the $CHOS^-$ ion is. Given that thioformic acid (TFA, CH(=O)SH) and its conjugate base ($CHOS^-$) are structurally similar to formic acid (HCOOH) and its conjugate base formate ($HCOO^-$), we may be able to use the condensed phase reactions of formate as an indicator of what the condensed phase fate of $CHOS^-$ is. By analogy to $HCOOH:HCOO^-$ chemistry, we propose two potential fates of thioformic acid; OH oxidation and evaporation.[30] The asymmetric nature to $TFA:CHOS^-$ would allow for two competing product distributions, $H_2S:HS^-$ + CO_2 and $H_2O:HO^-$ + OCS,[31,32] with the eventual fate of aqueous hydrogen sulfide (H_2S) ending as sulfate (SO_4^{2-}) through $^{\bullet}OH$ and ozone reactions.[33,34] The evaporation of thioformic acid could lead to a similar product distribution though OH oxidation in the gas phase rather than the aqueous phase.[35]

CONCLUSIONS AND ATMOSPHERIC IMPLICATIONS

We report measurements of γ(HPMTF) to dry sodium chloride (NaCl), wet NaCl, and wet sodium iodide (NaI) particles, with values of $(1.9 \pm 1.3) \times 10^{-4}$, $(1.6 \pm 0.6) \times 10^{-3}$, and $(9.2 \pm 2.3) \times 10^{-1}$, respectively. We find that HPMTF uptake is enhanced on deliquesced aerosol surfaces and

https://doi.org/10.1021/acs.jpca.2c03222
J. Phys. Chem. A XXXX, XXX, XXX−XXX

increased nucleophilicity of the species within the aerosol. Insights from the product ion distribution within the I^- CIMS suggest that the aqueous phase chemistry of HPMTF lead to the formation of H_2S, OCS and sulfate through a thioformic intermediate; however, focused investigations are needed to explore this chemistry.

Recent work evaluating the fate and atmospheric implications of HPMTF used an uptake value of 0.01 for HPMTF to marine aerosols, whose composition is primarily composed of sea salt ions (e.g., Na^+, Cl^-, and SO_4^{2-})[36,37] and cloud droplets in a global chemical transport model.[10] A 10-fold reduction in γ(HPMTF), as presented here, would lead to an overall decrease in the fraction of HPMTF that is lost to aerosol particles. Due to large cloud drop surface area and long in-cloud residence times, we do not expect the reduction in γ(HPMTF) reported here to impact modeled HPMTF loss to clouds. This is consistent with the direct measurements of rapid HPMTF cloud loss reported in Novak et al.[10]

The reactive uptake to and subsequent oxidation of HPMTF in marine aerosol may be different than that reported here for NaCl, due to variations in particle acidity and chemical composition.[38,39] Previous studies on uptake of carbonyl compounds[40−43] and a structurally similar molecule to HPMF (hydroperoxmethyl formate)[44] have shown that the reaction kinetics depend on both acidity and ionic strength. For this reason, we recommend additional laboratory work on the magnitude of uptake value and the product distribution of HPMTF to organic enriched, acidic, and chemically complex surfaces. In both Jernigan et al.[9] and Novak et al.,[10] it was assumed that HPMTF multiphase chemistry led to sulfate formation, arresting OCS formation in the OH-oxidation of HPMTF. Future work should explore the potential for production of OCS in the condensed-phase oxidation of HPMTF.

AUTHOR INFORMATION

Corresponding Author

Timothy H. Bertram − *Department of Chemistry, University of Wisconsin, Madison, Wisconsin 53706, United States;* orcid.org/0000-0002-3026-7588; Phone: (608) 890-3422; Email: timothy.bertram@wisc.edu

Authors

Christopher M. Jernigan − *Department of Chemistry, University of Wisconsin, Madison, Wisconsin 53706, United States*

Christopher D. Cappa − *Department of Civil and Environmental Engineering, University of California, Davis 95616 California, United States;* orcid.org/0000-0002-3528-3368

Complete contact information is available at: https://pubs.acs.org/10.1021/acs.jpca.2c03222

Author Contributions

Designed research, C.M.J. and T.H.B.; performed research, C.M.J.; contributed materials, T.H.B. and C.D.C.; analyzed data, C.M.J.; and wrote the paper, C.M.J., C.D.C., and T.H.B.

Notes

The authors declare no competing financial interest.

ACKNOWLEDGMENTS

This work was supported by the NSF Center for Aerosol Impacts on Chemistry of the Environment under Grant CHE 1801971.

REFERENCES

(1) Bates, T. S.; Lamb, B. K.; Guenther, A.; Dignon, J.; Stoiber, R. E. Sulfur Emissions to the Atmosphere from Natural Soures. *Journal of Atmospheric Chemistry* **1992**, *14* (1), 315−337.

(2) Lana, A.; Bell, T. G.; Simó, R.; Vallina, S. M.; Ballabrera-Poy, J.; Kettle, A. J.; Dachs, J.; Bopp, L.; Saltzman, E. S.; Stefels, J.; et al. An Updated Climatology of Surface Dimethlysulfide Concentrations and Emission Fluxes in the Global Ocean. *Global Biogeochemical Cycles* **2011**, *25* (1), 1−17.

(3) Vallina, S. M.; Simó, R.; Gassó, S. What Controls CCN Seasonality in the Southern Ocean? A Statistical Analysis Based on Satellite-Derived Chlorophyll and CCN and Model-Estimated OH Radical and Rainfall. *Global Biogeochemical Cycles* **2006**, *20* (1), GB1014.

(4) Korhonen, H.; Carslaw, K. S.; Spracklen, D. v.; Mann, G. W.; Woodhouse, M. T. Influence of Oceanic Dimethyl Sulfide Emissions on Cloud Condensation Nuclei Concentrations and Seasonality over the Remote Southern Hemisphere Oceans: A Global Model Study. *Journal of Geophysical Research Atmospheres* **2008**, *113* (15), 1−16.

(5) Galí, M.; Levasseur, M.; Devred, E.; Simó, R.; Babin, M. Sea-Surface Dimethylsulfide (DMS) Concentration from Satellite Data at Global and Regional Scales. *Biogeosciences* **2018**, *15* (11), 3497−3519.

(6) Carslaw, K. S.; Lee, L. A.; Reddington, C. L.; Pringle, K. J.; Rap, A.; Forster, P. M.; Mann, G. W.; Spracklen, D. v.; Woodhouse, M. T.; Regayre, L. A.; et al. Large Contribution of Natural Aerosols to Uncertainty in Indirect Forcing. *Nature* **2013**, *503* (7474), 67−71.

(7) Veres, P. R.; Neuman, J. A.; Bertram, T. H.; Assaf, E.; Wolfe, G. M.; Williamson, C. J.; Weinzierl, B.; Tilmes, S.; Thompson, C. R.; Thames, A. B.; et al. Global Airborne Sampling Reveals a Previously Unobserved Dimethyl Sulfide Oxidation Mechanism in the Marine Atmosphere. *Proc. Natl. Acad. Sci. U. S. A.* **2020**, *117* (9), 4505−4510.

(8) Vermeuel, M. P.; Novak, G. A.; Jernigan, C. M.; Bertram, T. H. Diel Profile of Hydroperoxymethyl Thioformate: Evidence for Surface Deposition and Multiphase Chemistry. *Environmental Science Technology* **2020**, *54*, 12521−12529.

(9) Jernigan, C. M.; Fite, C. H.; Vereecken, L.; Berkelhammer, M. B.; Rollins, A. W.; Rickly, P. S.; Novelli, A.; Taraborrelli, D.; Holmes, C. D.; Bertram, T. H. Efficient Production of Carbonyl Sulfide in the Low-NO x Oxidation of Dimethyl Sulfide. *Geophys. Res. Lett.* **2022**, *49* (3), e2021GL096838.

(10) Novak, G. A.; Fite, C. H.; Holmes, C. D.; Veres, P. R.; Neuman, J. A.; Faloona, I.; Thornton, J. A.; Wolfe, G. M.; Vermeuel, M. P.; Jernigan, C. M.; et al. Rapid Cloud Removal of Dimethyl Sulfide Oxidation Products Limits SO 2 and Cloud Condensation Nuclei Production in the Marine Atmosphere. *Proc. Natl. Acad. Sci. U. S. A.* **2021**, *118* (42), e2110472118.

(11) Fung, K. M.; Heald, C.; Kroll, J.; Wang, S.; Jo, D.; Gettelman, A.; Lu, Z.; Liu, X.; Zaveri, R.; Apel, E.; Blake, D.; et al. Exploring DMS Oxidation and Implications for Global Aerosol Radiative Forcing. *Atmospheric Chemistry and Physics* **2022**, *22*, 1549−1573.

(12) Khan, M. A. H.; Bannan, T. J.; Holland, R.; Shallcross, D. E.; Archibald, A. T.; Matthews, E.; Back, A.; Allan, J.; Coe, H.; Artaxo, P.; Percival, C. J. Impacts of Hydroperoxymethyl Thioformate on the Global Marine Sulfur Budget. *ACS Earth Space Chem.* **2021**, *5* (10), 2577−2586.

(13) Vermeuel, M. P.; Novak, G. A.; Jernigan, C. M.; Bertram, T. H. Diel Profile of Hydroperoxymethyl Thioformate: Evidence for Surface Deposition and Multiphase Chemistry. *Environ. Sci. Technol.* **2020**, *54* (19), 12521−12529.

(14) Bertram, T. H.; Thornton, J. A.; Riedel, T. P. An Experimental Technique for the Direct Measurement of N_2O_5 Reactivity on Ambient Particles. *Atmospheric Measurement Techniques Discussions* **2009**, *2* (1), 231−242.

(15) Laskina, O.; Morris, H. S.; Grandquist, J. R.; Qin, Z.; Stone, E. A.; Tivanski, A. v; Grassian, V. H. Size Matters in the Water Uptake and Hygroscopic Growth of Atmospherically Relevant Multicomponent Aerosol Particles. *J. Phys. Chem. A* **2015**, *119* (19), 4489−4497.
(16) Miñambres, L.; Méndez, E.; Sánchez, M. N.; Castaño, F.; Basterretxea, F. J. The Effect of Low Solubility Organic Acids on the Hygroscopicity of Sodium Halide Aerosols. *Atmospheric Chemistry and Physics* **2014**, *14* (20), 11409−11425.
(17) Weis, D. D.; Ewing, G. E. Water Content and Morphology of Sodium Chloride Aerosol Particles. *Journal of Geophysical Research: Atmospheres* **1999**, *104* (D17), 21275−21285.
(18) Biskos, G.; Malinowski, A.; Russell, L. M.; Buseck, P. R.; Martin, S. T. Nanosize Effect on the Deliquescence and the Efflorescence of Sodium Chloride Particles. *Aerosol Sci. Technol.* **2006**, *40* (2), 97−106.
(19) Pinterich, T.; Spielman, S. R.; Wang, Y.; Hering, S. v; Wang, J. A Humidity-Controlled Fast Integrated Mobility Spectrometer (HFIMS) for Rapid Measurements of Particle Hygroscopic Growth. *Atmos. Meas. Technol.* **2017**, *10* (12), 4915−4925.
(20) Miñambres, L.; Méndez, E.; Sánchez, M. N.; Castaño, F.; Basterretxea, F. J. Water Uptake Properties of Internally Mixed Sodium Halide and Succinic Acid Particles. *Atmos. Environ.* **2011**, *45* (32), 5896−5902.
(21) Fuchs, N. A.; Sutugin, A. G. High-Dispersed Aerosols. *Topics in current aerosol research* **1971**, 1.
(22) Hanson, D.; Kosciuch, E. The NH3Mass Accommodation Coefficient for Uptake onto Sulfuric Acid Solutions. *J. Phys. Chem. A* **2003**, *107* (13), 2199−2208.
(23) Cadle, R. D.; Huff, H. The The Oxidation of Iodide to Iodine by Dilute Solutions of Organic Peroxides. *J. Phys. Chem.* **1950**, *54* (8), 1191−1195.
(24) Garland, J. A.; Curtis, H. Emission of Iodine from the Sea Surface in the Presence of Ozone. *Journal of Geophysical Research: Oceans* **1981**, *86* (C4), 3183−3186.
(25) Rouvière, A.; Sosedova, Y.; Ammann, M. Uptake of Ozone to Deliquesced KI and Mixed KI/NaCl Aerosol Particles. *J. Phys. Chem. A* **2010**, *114* (26), 7085−7093.
(26) Lowry, T. H.; Richardson, K. S. *Mechanism and Theory in Organic Chemistry*; Harper & Row: New York, 1987; p 294
(27) Staudt, S., *Heterogeneous Reactions of Nocturnal Nitrogen Oxides at Atmospherically Relevant Aqueous Interfaces*; Thesis, 2019.
(28) Lopez-Hilfiker, F. D.; Iyer, S.; Mohr, C.; Lee, B. H.; D'Ambro, E. L.; Kurtén, T.; Thornton, J. A. Constraining the Sensitivity of Iodide Adduct Chemical Ionization Mass Spectrometry to Multifunctional Organic Molecules Using the Collision Limit and Thermodynamic Stability of Iodide Ion Adducts. *Atmospheric Measurement Techniques* **2016**, *9* (4), 1505−1512.
(29) Brophy, P.; Farmer, D. K. Clustering, Methodology, and Mechanistic Insights into Acetate Chemical Ionization Using High-Resolution Time-of-Flight Mass Spectrometry. *Atmospheric Measurement Techniques* **2016**, *9* (8), 3969−3986.
(30) Chameides, W. L.; Davis, D. D. Aqueous-Phase Source of Formic Acid in Clouds. *Nature* **1983**, *304* (5925), 427−429.
(31) Jacob, D. J. Chemistry of OH in Remote Clouds and Its Role in the Production of Formic Acid and Peroxymonosulfate. *Journal of Geophysical Research: Atmospheres* **1986**, *91* (D9), 9807−9826.
(32) Anbar, M.; Neta, P. A Compilation of Specific Bimolecular Rate Constants for the Reactions of Hydrated Electrons, Hydrogen Atoms and Hydroxyl Radicals with Inorganic and Organic Compounds in Aqueous Solution. *International Journal of Applied Radiation and Isotopes* **1967**, *18* (7), 493−523.
(33) Zhang, J.-Z.; Millero, F. J. The Products from the Oxidation of H2S in Seawater. *Geochim. Cosmochim. Acta* **1993**, *57* (8), 1705−1718.
(34) Hoigné, J.; Bader, H.; Haag, W. R.; Staehelin, J. Rate Constants of Reactions of Ozone with Organic and Inorganic Compounds in Water—III. Inorganic Compounds and Radicals. *Water Res.* **1985**, *19* (8), 993−1004.
(35) Wine, P. H.; Astalos, R. J.; Mauldin III, R. L. Kinetic and Mechanistic Study of the Hydroxyl+ Formic Acid Reaction. *J. Phys. Chem.* **1985**, *89* (12), 2620−2624.
(36) Xiao, H.-W.; Xiao, H.-Y.; Shen, C.-Y.; Zhang, Z.-Y.; Long, A.-M. Chemical Composition and Sources of Marine Aerosol over the Western North Pacific Ocean in Winter. *Atmosphere* **2018**, *9*, 298.
(37) O'Dowd, C. D.; de Leeuw, G. Marine Aerosol Production: A Review of the Current Knowledge. *Philosophical Transactions of the Royal Society A: Mathematical, Physical and Engineering Sciences* **2007**, *365* (1856), 1753−1774.
(38) Angle, K. J.; Crocker, D. R.; Simpson, R. M. C.; Mayer, K. J.; Garofalo, L. A.; Moore, A. N.; Mora Garcia, S. L.; Or, V. W.; Srinivasan, S.; Farhan, M.; et al. Acidity across the Interface from the Ocean Surface to Sea Spray Aerosol. *Proc. Natl. Acad. Sci. U. S. A.* **2021**, *118* (2), e2018397118.
(39) Bertram, T. H.; Cochran, R. E.; Grassian, V. H.; Stone, E. A. Sea Spray Aerosol Chemical Composition: Elemental and Molecular Mimics for Laboratory Studies of Heterogeneous and Multiphase Reactions. *Chem. Soc. Rev.* **2018**, *47* (7), 2374−2400.
(40) Wu, Q. Q.; Huang, L. B.; Liang, H.; Zhao, Y.; Huang, D.; Chen, Z. M. Heterogeneous Reaction of Peroxyacetic Acid and Hydrogen Peroxide on Ambient Aerosol Particles under Dry and Humid Conditions: Kinetics, Mechanism and Implications. *Atmospheric Chemistry and Physics* **2015**, *15* (12), 6851−6866.
(41) Liggio, J.; Li, S. M. Reactive Uptake of Pinonaldehyde on Acidic Aerosols. *Journal of Geophysical Research Atmospheres* **2006**, *111* (24), 1−12.
(42) Kroll, J. H.; Ng, N. L.; Murphy, S. M.; Varutbangkul, V.; Flagan, R. C.; Seinfeld, J. H. Chamber Studies of Secondary Organic Aerosol Growth by Reactive Uptake of Simple Carbonyl Compounds. *Journal of Geophysical Research Atmospheres* **2005**, *110* (23), 1−10.
(43) Liggio, J.; Li, S. M.; McLaren, R. Reactive Uptake of Glyoxal by Particulate Matter. *Journal of Geophysical Research D: Atmospheres* **2005**, *110* (10), 1−13.
(44) Thamm, J.; Wolff, S.; Turner, W. v; Gäb, S.; Thomas, W.; Zabel, F.; Fink, E. H.; Becker, K. H. Proof of the Formation of Hydroperoxymethyl Formate in the Ozonolysis of Ethene: Synthesis and FT-IR Spectra of the Authentic Compound. *Chem. Phys. Lett.* **1996**, *258* (1), 155−158.

https://doi.org/10.1021/acs.jpca.2c03222
J. Phys. Chem. A XXXX, XXX, XXX−XXX